Macromolecules

ARTICLE

pubs.acs.org/Macromolecules

Electropolymerized Molecularly Imprinted Polymer Film: EIS Sensing of Bisphenol A

Dahlia C. Apodaca,[†,‡] Roderick B. Pernites,[†] Ramakrishna Ponnapati,[†] Florian R. Del Mundo,[‡] and Rigoberto C. Advincula*[,†,‡]

[†]Department of Chemistry and Department of Chemical and Biomolecular Engineering, University of Houston, Houston, Texas 77204-5003, United States

[‡]Institute of Chemistry, University of the Philippines, Diliman, Quezon City Philippines 1101

Supporting Information

ABSTRACT: Bisphenol A (BPA) sensing was investigated based on electrochemical impedance spectroscopy (EIS) measurements of an electropolymerized molecularly imprinted polymer (E-MIP) film. The E-MIP film is composed of varying ratios of BPA−terthiophene and carbazole monomer complex deposited onto indium tin oxide (ITO) substrates via anodic electropolymerization using cyclic voltammetry (CV). Subsequently, the interfacial properties of these films were studied using the non-Faradaic EIS technique. The same technique was then used to measure the presence of templated BPA which is a known endocrine disrupting chemical (EDC). Analyses of the EIS results were performed using equivalent circuits in order to model the electrical and impedance properties through the interface. A linear calibration curve was established in the range 0−12 mM concentrations of the analyte. Moreover, the selectivity of the films against bisphenol AF and diphenolic acid was demonstrated. The E-MIP sensor may have advantages in environmental monitoring of bisphenol A in aqueous analyte/pollutant samples.

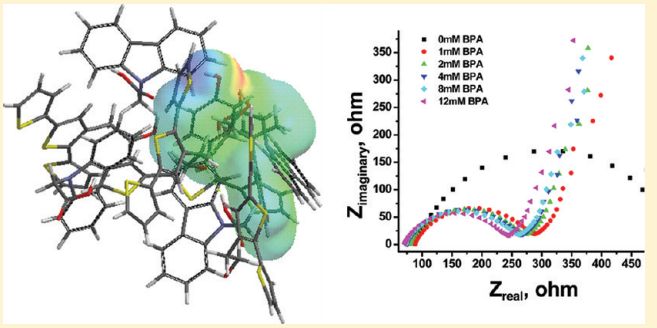

INTRODUCTION

Bisphenol A (2,2-bis(4-hydroxyphenyl)propane) or BPA is a chemical of particular importance because of its extensive use in industry. It is primarily used in the production of plastics mainly polycarbonate and epoxy resins and as an additive. Owing to the high use of BPA in manufacturing consumer products, high levels are expected in surface and industrial wastewaters. Reports have indicated the health risk posed by exposure to significant levels of BPA since it exhibits an estrogen-like activity.[1] Its high blood levels in men and women are associated with reproduction dysfunction, endometrial hyperplasia, recurrent miscarriages, abnormal karyotypes, and polycystic ovarian syndrome, a health hazard to both infant and the general population.[2] Gas chromatography coupled with mass spectroscopy (GC-MS) and high performance liquid chromatography (HPLC) has been commonly used for quantitative determination of BPA in environmental water and packaged food product samples. These methods require several sample preparation steps including extraction and preconcentration. Immunoaffinity chromatography is also useful for the extraction of endocrine disrupting chemicals (EDC)s and pesticide residues. Most of the reported immunoaffinity columns use polyclonal and monoclonal antibodies. However, these types of antibodies can be difficult to reproduce in large quantities and can interfere with the antigen-binding reactions. While analytically useful, these techniques cannot meet the demand to regularly monitor the level of processing additives that may end up as pollutants. This necessitates the development of alternative and portable analytical methods including the development of chemical and biosensors to fill the need.

Molecular recognition or artificial receptors with molecularly imprinted polymers (MIP) has been a significant tool for the development of micro- and multianalyte sensors.[3−8] Binding of the target analyte with the polymer network is made possible by the formation of shape-complementary cavities. The MIP technique is an effective and robust method for obtaining a recognition element for incorporation in chemical and biological sensors.[9] MIPs are usually prepared via the traditional bulk polymerization of functional monomer, template, and cross-linker in the presence of a porogen. In bulk polymerization, it is imperative that the functional monomer must have a considerable interaction with the template in order to achieve good imprinting. Moreover, a cross-linker is commonly included in order to fix the functional monomers in place and keep the binding cavities intact. Choices for cross-linkers in vinyl free-radical

Received: May 7, 2011
Revised: August 1, 2011
Published: August 15, 2011

polymerization generally include ethylene glycol dimethacrylate (EGDMA), divinylbenzene (DVB), trimethylolpropane trimethacrylate (TRIM), and others. While this particular method and materials has been widely used in MIPs for chromatographic separation, surface imprinting has proven to be a challenge for polymer films used as recognition elements in flat surface transduced chemical and biological sensors. There are several considerations: (1) molecular recognition is a function of the surface chemistry at the polymer−template interface, (2) the generation of signal resulting from the detection of template is significantly enhanced when the MIP is directly interfaced on the transducer's surface, and (3) analyte binding is both a function of porosity and gradient affinity (adsorption) to the film. In principle, an imprinted polymer can be grown directly from a surface with a chemically or physically adsorbed initiator, a technique demonstrated by Schweitz.[10] Living/controlled polymerization techniques have also been employed to produce an imprinted polymer from the surface.[11] Sellergren and co-workers modified a surface with a photosensitive dithiocarbamate which functions as an iniferter.[12] On the other hand, Malitesta et al.[13] reported very thin molecularly imprinted film on a gold-coated quartz crystal (QCM) by electropolymerization of phenols and aromatic amines.

In general, imprinting electropolymerization may prove advantageous especially matters that concern mass transfer and accessibility by enabling the direct immobilization of the polymer matrix film onto the transducer's surface and allowing control over film thickness. These factors are regarded to be very important in achieving the desired sensitivity of a sensor. Early reports of glucose oxidase entrapped in polypyrrole[14] paved the way for the use of conducting polymers in the development of biosensors, with the potential benefit of an enhanced charge transport across the polymer matrix. Guo et al.[15] investigated the adhesion/spreading and proliferation of mammalian cells on electropolymerized porphyrin films for biosensing applications. In their work, sufficient hydrophilicity for cell attachment was observed and that the QCM technique was successfully applied for monitoring cell growth for real time, continuous, and on line monitoring. Zhang et al.[16] focused their attention to the utilization of a polypyrrole graft copolymer, poly(styrenesulfonic acid-*graft*-pyrrole), to functionalize reduced graphene oxide via $\pi-\pi$ noncovalent interactions in the fabrication of an electrocatalytic biosensor. The biosensor is intended to be used for the determination of hypoxanthine, a good indicator of fish products freshness in food industries. The determination of hypoxanthine in this biosensor was achieved by measuring the oxidation current of hydrogen peroxide and uric acid at the electrode interface. While Zhang et al. made use of a grafted copolymer for the determination of hypoxanthine, Choi et al.[17] reported the use of SPR in the detection of mycoestrogen zearalenone with the electropolymerized molecularly imprinted polypyrrole film as the recognition system. In particular, a shift from 85.702° to 85.917° has been observed when 3000 ng/mL of the analyte was injected into the SPR cell and saturation was observed after 40 min. Despite the number of strategies employed for the preparation of imprinted polymers on surfaces, a standard protocol is yet to be established for surface molecular imprinting with respect to electropolymerized conducting polymers.

Conjugated polymers are amenable to surface MIP due to their electropolymerizability and doping−dedoping or redox reversibility properties.[18] Like polypyrrole and polyaniline, polythiophenes can be both oxidatively or reductively doped in a proper solvent.[19] The presence of sulfur in polythiophenes also enables it to be reduced and thus n-doped.[33] Moreover, the electron density distribution of the thiophene ring in the presence of other functional groups enhances the reactivity of the thiophene monomer.[20] There have been a number of studies on electrochemically prepared polythiophene films for sensing applications.[21] On the other hand, the use of carbazole has gained considerable attention since the discovery of photoconductivity in poly(*N*-vinylcarbazole) (PVK) by Hoegl.[22] Carbazole-based polymers exhibit properties such as formation of relatively stable radical cations (holes), high-charge carrier mobilities, and high thermal and photochemical stability.[23] Moreover, carbazoles have been studied as photoconductive polymers and organic photoreceptors.[24]

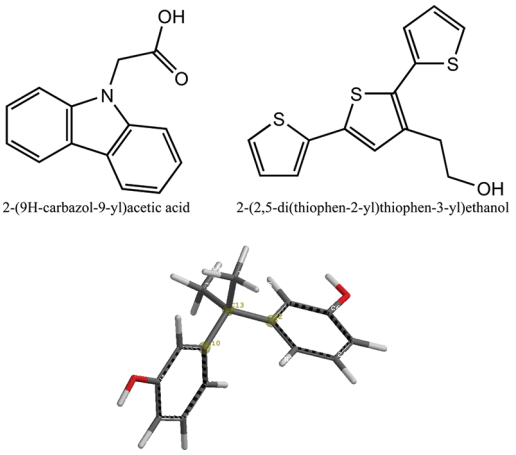

Figure 1. Structures of the carbazole and terthiophene monomers used in this study and a molecular model representation of (2,2-bis(4-hydroxyphenyl)propane) or bisphenol A (see Figure S1 for BPA−monomer complexation modeling studies in the Supporting Information).

In this study, we have utilized the anodic electropolymerization of both terthiophene and carbazole monomers to prepare electropolymerized MIPs (E-MIPs) for the detection of BPA. The monomer 2-(2,5-di(thiophen-2-yl)thiophen-3-yl)ethanol or simply labeled as G0 3TOH is a terthiophene-based π-conjugated monomer. Since, it has been established that the polymer morphology is also affected by the stoichiometry and the concentration of the template and monomer,[8] we have also investigated the effect of copolymerization of G0 3TOH with carbazole, 2-(9*H*-carbazol-9-yl)acetic acid. The design of the polymer network composition should complement the size, shape, and orientation of the monomer functional group to the imprint template. The intrinsic conductivity, stability, and processabiltiy of both the terthiophene and the carbazole monomers in both doped and neutral states[25] make them good candidates for the preparation of imprinted polymers via coelectropolymerization. Their quantitative coelectropolymerization has been previously demonstrated by us resulting in smooth film formation and a high degree of compatibilization.[26] The chemical structures of the functional monomers utilized in this study are shown in Figure 1 (see Figure S1 for monomer−BPA modeling).

Although a range of MIP-based chemosensors have already been reported,[27] the electrochemical approach in tandem with the MIP protocol process has not been largely explored because of issues pertaining to homogeneous film formation and difficulty in *in situ* characterization.[28] Also, the possible interference or degradation of the template/analyte with the electropolymerization

process is a main concern. It is therefore important to develop E-MIP methods in which templating is efficient and an *in situ* monitoring method be employed with electrodeposition. In previous studies, electrochemistry coupled with the QCM or E-QCM was employed for the *in situ* growth monitoring of the MIP films on a gold electrode surface as well as for analyte sensing.[7,29] The E-QCM technique permitted the simultaneous monitoring of the frequency (mass) and the viscoelastic behavior of the film during electrodeposition.[30] Also, the $I-V$ or $I-T$ (current vs time) measurements were recorded on the same Au-QCM electrode. Another method that has been shown to be useful for this type of application is the electrochemical surface plasmon resonance spectroscopy or EC-SPR.[8]

Thus, we present a protocol for depositing E-MIP films based on copolymers of terthiophene and carbazole derivatives utilizing electrochemical impedance spectroscopy (EIS) to generate a BPA sensor. In this case, an advantage is that an electropolymerized film brings about a network film containing cavities for the binding of BPA without the use of an added cross-linker.[8] The sensitivity and selectivity of the E-MIP film toward BPA were determined using the EIS technique. EIS is yet to be demonstrated as an effective and robust method for investigating electrode processes, for determining the surface adsorption kinetics and mass-transport parameters, and for adopting smaller electrochemical perturbations for analyte detection in sensors.[31]

EXPERIMENTAL SECTION

Chemicals. 2-(9*H*-Carbazol-9-yl)acetic acid (labeled as CbzCOOH), bisphenol A, tetrabutylammonium hexafluorophosphate (TBAH), bisphenol AF, and diphenolic acid were purchased from Sigma-Aldrich and VWR. All chemicals were used as received. Aqueous solutions were prepared from water purified using a Millipore system (resistivity 18.2 MΩ·cm). The synthesis of the G0 3TOH is as follows:[32,31] the synthesis of ethyl 2-(2,5-di(thiophen-2-yl)thiophen-3-yl)acetate (3T ET) was carried out by first synthesizing ethyl 2-(2,5-dibromothiophen-3-yl)-acetate as reported in the literature.[25] Ethyl 2-(2,5-dibromothiophen-3-yl)-acetate and 2-(tributylstanny1)thiophene were then added to a dry DMF solution of dichlorobis(tripheny1phosphine)palladium. After three freeze−thaw cycles, the mixture was heated at 100 °C for 48 h. The mixture was cooled to room temperature and poured into a beaker containing 150 mL of water and subsequently extracted with CH_2Cl_2. The compound 3T ET was reduced under the following conditions: 10 mL of THF was added, dropwise, under nitrogen to an ice-cooled 100 mL THF suspension of $LiAlH_4$, to yield 2-(2,5-di(thiophen-2-yl)thiophen-3-yl)-ethanol (G0 3TOH). In principle, the dendron synthesis can be carried out to succeeding generations, G2, G3, G4, ..., as needed in an AB_2 convergent manner.[18,33]

Instrumentation. Cyclic voltammetry (CV) was performed on an Autolab General Purpose Electrochemical System (GPES) PGSTAT12 module with a three-electrode cell. GPES software was used to run data acquisition. Electropolymerization were performed on gold-coated glass slides or indium tin oxide (ITO) surfaces which were cleaned according to the following protocol: The gold-coated glass slide were cleaned in piranha solution for 60 s (H_2O_2/H_2SO_4, 1:3, v/v), whereas 3 × 1.5 cm cut ITO slides were washed with Alconox (Sparkleen) and were subsequently rinsed and sonicated in Milli-Q water for 5 min. Successive washing in different solvents ensued, namely, in isopropyl alcohol, hexane, and toluene, in which each washing was accompanied by 10 min sonication. Both gold and ITO slides were then subjected to plasma cleaning using a March Plasmod GCM 200 for 300 s at 10 W with an Ar gas purge.

This electrochemical set up is also equipped with a Frequency Response Analyzer module (FRA). The FRA hardware consists of a digital signal generator module, a signal conditioning unit, and a fast analog-to-digital converter with two channels. The Fit and Simulation version 1.7, built in the FRA software, allowed the fitting of the circuit parameters to the measured data using the nonlinear least-squares method. EIS sensing was done by monitoring actual kinetic curves. A typical measurement for comparison was done with 0−12 mM concentrations of BPA in acetonitrile. Various concentrations were specified for sensitivity studies. The EIS curve was recorded three times.

For X-ray photoelectron spectroscopy (XPS), photoelectrons were collected on a Physical Electronics Model 5700 XPS instrument using a monochromatic Al Kα X-ray source (1486.6 eV) operated at 350 W. The analyzed area, collection solid cone, and take off angle were set at 800 mm, 5°, and 45°, respectively. A pass energy of 11.75 eV was employed, resulting in an energy resolution of better than 0.51 eV. All spectra were acquired in vacuum (5×10^{-9} Torr or better) and at room temperature. A Shirley background subtraction routine was applied throughout the experiment. The binding energy scale was calibrated prior to analysis using the Au $4f_{7/2}$ line. Charge neutralization was ensured through cobombardment of the irradiated area with an electron beam. Data processing was carried out using the Multipak software package.

Ellipsometry measurements were conducted using the OPTREL-Multiskop at an angle of 60° with respect to the surface normal and at a fixed wavelength of 632.8 nm. Δ and ψ values were obtained for the polymer films and the clean gold-coated quartz crystal surface. The ellipsometry data were then fitted using a fitting program (Elli, Optrel), assuming a refractive index (RI) of 1.5 for the polymer layer.[34]

UV−vis spectroscopy measurements were carried out on a Perkin-Elmer Lambda 20. Fluorescence spectra were obtained in a Perkin-Elmer LS50B spectrometer using 250 nm excitation.

RESULTS AND DISCUSSION

***In Situ* CV Deposition of Imprinted and Nonimprinted Copolymer Films.** In contrast to our previous report[7] in which a terthiophene dendron was only used for the imprinting of folic acid, this study has explored the use of another π-conjugated monomer, to be codeposited with the G0 3TOH terthiophene monomer in certain ratios. We speculated that the amount of specific binding cavities from electropolymerized film can be adjusted with the addition of another conducting monomer containing additional functional group. The approach was to introduce a carbazole containing −COOH moiety to generate a receptor capable of immobilizing more template molecules via noncovalent interactions present in the prepolymerization mixture. In this manner, the quantity and quality of resulting E-MIP recognition sites may be enhanced. The imprinted copolymer film was prepared by *in situ* CV deposition on the surface of ITO. The technique allows for the preparation of films with varying thickness by CV and directly interfaces the imprinted polymer onto the surface of a working electrode which can also be interfaced to an EIS system. The potential window, number of cyclic scans, and polymer composition were optimized to establish the most appropriate conditions in obtaining the best film that will exhibit high sensitivity and selectivity toward BPA. Polymerization was typically conducted by cycling the potential from 0 to 1.1 V at a scan rate of 50 mV/s for ten times (10 cycles). The E-MIP film was prepared from a 50 μM solution of monomers and 5 mM BPA complex in acetonitrile (ACN) containing 0.1 M of tetrabutylammonium hexafluorophosphate (TBAH) as supporting electrolyte. A control polymer film, i.e.,

Table 1. Molar Ratio of the CbzCOOH and G0 3TOH Monomers in the Prepolymer Solutions Used in the Electropolymerization of Imprinted (with Bisphenol A) and Nonimprinted (without Bisphenol A) Polymer Films

prepolymer solution	CbzCOOH concn (μM)	G0 3TOH concn (μM)
1	50	
2		50
3	25	75
4	50	50
5	75	25

the nonimprinted polymer (NIP) film, was prepared under the same conditions but in the absence of the template (bisphenol A). Table 1 gives the details on the monomer composition used to prepare the imprinted and nonimprinted electropolymerized films.

In a typical CV experiment, the film formation was monitored through changes in current per cycle. At each CV cycle, the oxidation current increases, suggesting a stepwise growth of the polymer film on the substrate's surface. The electrochemical polymerization represents a statistical reaction between the terthiophene units and the carbazole group resulting to further cross-linking.[35] The term cross-linking refers to the ability of the monomer−template complex to enable terthiophene−terthiophene, terthiophene−carbazole, and carbazole−carbazole reactivity, intra- or intermolecularly. During the electropolymerization process, the formation of linear polymeric or oligomeric species is also possible from free terthiophene and carbazole units. The dual function of the monomers, i.e., as functional monomers and as cross-linkers, is regarded to be responsible for the generation of binding cavities that complement the size and shape of BPA, which enhances the sensing capability of the polymer. Hence, it was significant to look at the effect of varying polymer composition of the imprinted polymer film upon binding of BPA. Variations in the polymer composition was performed by electropolymerizing different molar ratios of G0 3TOH and CbzCOOH (Table 1). Each resulting film was characterized and compared to films prepared from only one monomer, i.e., either G0 3TOH or CbzCOOH only.

The growth formation of each polymer film was characterized by CV. Figure 1 gives the voltammogram for 75 μM G0 3TOH and 25 μM CBzCOOH copolymer film composition. The CV of the other different molar ratios of G0 3TOH and CbzCOOH are shown in the Supporting Information.

As shown in the voltammograms, film formation for the imprinted polymer was different from the growth formation of the nonimprinted polymer film. The deposition of the imprinted polymers resulted to a relatively higher increase in anodic peak current compared with the nonimprinted films. This evidently shows that the presence of BPA enhanced the cross-linking of the monomers, resulting in a much higher current density. The polymer films containing a higher amount of G0 3TOH tend to give a moderately higher oxidation peak current (Supporting Information, Figure S2). This leads to the assumption of distinct structures between the E-MIP and the NIP films and that higher density films were obtained from imprinted films compared to nonimprinted films. It is also noteworthy to discuss the observed changes in the doping behavior of the formed conjugated polymer backbone which may have been influenced by the prepolymer complexation of the template with the monomers.

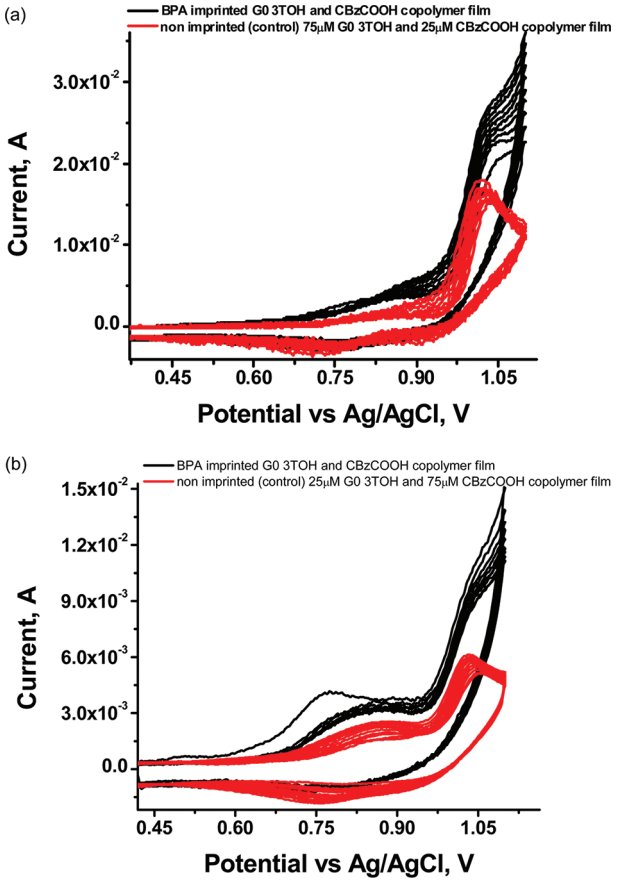

Figure 2. Cyclic voltammograms of the imprinted and nonimprinted copolymer films: (a) 75 μM GO 3TOH and 25 μM CBzCOOH; (b) 25 μM G0 3TOH and 75 μM CbzCOOH. Potential cycling from 0 to 1.1 V at a scan rate of 50 mV/s for 10 cycles with 0.1 M of TBAH as supporting electrolyte.

The anodic peak potentials were found to have shifted after the 10th cycle of deposition of the E-MIP compared to the nonimprinted films on the ITO surface. This suggests that incorporation of the BPA may have caused conformational changes on the polymer backbone brought about by more H-bonding and other possible noncovalent interactions between the template and the monomer. Moreover, it may be speculated that transitions observed in the peak potential have led to the formation of polymer networks that are highly cross-linked and yet with a lower extent of π-conjugation depending on the respective amount of G0 3TOH or CbzCOOH present in the film.[26,36]

The UV−vis spectroscopy technique was also employed in this study to ascertain the changes in the π-conjugation of the electrocopolymerized films formed after electrochemical deposition on ITO. A shift in the absorption maximum to longer wavelength signifies greater π-conjugation. On the other hand, it can be assumed that the polymer backbone conformation is more disordered (twisted) if the absorption maximum is shifted to shorter wavelength. To illustrate this point, the UV−vis spectra of the G0 3TOH films were compared (Figure 3). It is assumed that in the presence of BPA conformational changes may have occurred due to numerous intermolecular interactions between functional groups of BPA and that of the polymer. Such causes a decrease in π-conjugation and a more aggregated structure of the formed polythiophene−polycarbazole resulting to a slight shift

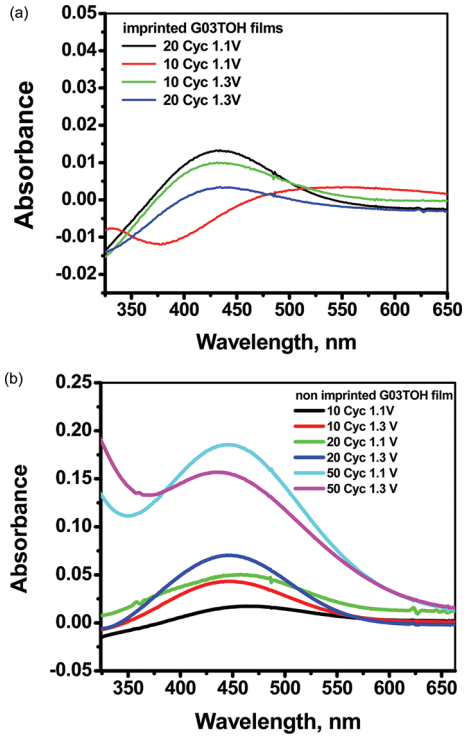

Figure 3. UV−vis spectra of the (a) imprinted (MIP) and (b) nonimprinted (NIP) G0 3TOH films. Films were electrodeposited on ITO via CV employing two potential scan windows: 0−1.1 and 0−1.3 V.

in the λ_{max} to shorter wavelength (blue shift) and to decrease in intensity (hypochromic shift). This was indeed observed in the case of the E-MIP film. The observed hypochromic shift may be attributed to the occurrence of more conformational defects disrupting the π-conjugation within the polymer structure compared to the NIP films. This is a consequence of the presence of the BPA in the matrix affording a more conformationally disordered backbone and networked structure. The energetics of the BPA−copolymer interaction could have exceeded that of the π-orbital overlap of the resulting polymer backbone causing the twisting of the polymer structure.[37] In a parallel study, Leclerc et al.[38] were also able to observe a blue shift in the polymer backbone absorption upon binding of the avidin to the biotin containing polythiophene.

As with the case of the UV absorption of electropolymerized NIP film, in the absence of the template molecules, the electropolymerized NIP film may have adopted a more planar and a much longer polymer backbone compared with the electropolymerized MIP film as indicated by slight shift in the λ_{max} to longer wavelength. Polymers with longer chain lengths are thus expected to manifest changes in its absorption spectrum brought about by inter- and intrachain interactions during film organization occurring from solution to solid substrate. Longer chain lengths easily induce chain−chain contacts as well as random chemical defects[39] which, as a result, led to the formation of a few aggregates and other supramolecular structures such as low-energy excitons,[40] which affect the resulting optical properties of the polymer film.

We also attempted to explain the observations generated from the CV experiments using the *in situ* E-QCM technique. With the E-QCM technique, it is possible to correlate electrochemically induced mass changes on the quartz crystal electrode per CV cycle. Simultaneous with the reduction and oxidation peaks on the voltammograms, the changes in frequency can be recorded from the QCM. Adopting the electrochemically stimulated conformational relaxation (ESCR) model developed by Otero et al.[41] to explain for the observed E-QCM data, we also considered that the polymer film expands upon the application of anodic potential due to insertion of the hexafluorophosphate counterions as well as of BPA molecules into the polymer network. This results to a corresponding decrease in the frequency due to an increase in mass attributable to polymer growth parallel to the metal surface. As also explained by Otero's group, the growth of polymer is controlled by a structural relaxation involving conformational changes of polymer segment and a swelling of the polymer due to electrostatic repulsion between the chains and to incorporations of counterions and BPA molecules. On the other hand, during the cathodic cycle (reduction), the change in the frequency (increase) is due to dedoping of ions, signaling a decrease in mass due to shrinking of the polymer. As the polymerization progresses through repeated cycling of the potential, the diffusion of the counterions and BPA molecules became more difficult due to cross-linking, enabling the deposition of suitable number of template molecules within the polymer network. This can be equated to the formation of suitable number of binding sites for the subsequent rebinding of BPA molecules. The changes in frequency can then be translated into the corresponding deposited mass of the polymer film adsorbed on the surface through the Sauerbrey equation[42]

$$\Delta f = -2f_0^2 \Delta m / A(\rho_q \mu_q)^{1/2} \quad (1)$$

where f_0 is the fundamental resonant frequency of the QCM (5 MHz), A is the area of the electrode (1.327 cm^2), ρ_q is the density of the quartz (2.65 g/cm^3), and μ_q is the shear modulus of the quartz (2.95×10^6 N/cm^2).

Figure S3 (Supporting Information) depicts the progress of electropolymerization (raw data) of the imprinted and nonimprinted (control) polymer films on gold-coated quartz crystal. As illustrated in the plot, the electrochemical deposition of polymers after 10 CV cycles brings about the formation of polymer films as indicated by a large shift on the frequency of the quartz crystal. In both plots, it was shown that a relatively denser film was obtained when the template (BPA) was incorporated in the prepolymer mix (E-MIP). These correspond to a higher surface mass density for the imprinted polymer films relative to the nonimprinted films, regardless of the polymer composition. However, the mass deposition is generally well-behaved for the electrochemical deposition of the imprinted copolymer films, which resulted in the observed linear growth rate coincident with a highly reversible redox behavior for the film. In view of the foregoing discussion, the use of conducting polymers for E-MIP preparation proved to be advantageous as their electrochemical properties can be modulated due to template−polymer association and variations in its oxidation−reduction state may induce changes in its complexation behavior[43] to permit an enhanced sensing capability for the E-MIP film toward BPA molecules, as interpreted from the E-QCM, CV, and UV data.

Characterization of the Imprinted and Nonimprinted Copolymer Films. The effect of polymer composition was investigated in the preparation of the E-MIP as this may eventually affect the structural integrity of the resulting film and sensor performance.[44] It has been previously pointed out that an E-MIP film must possess a reasonable mechanical stability

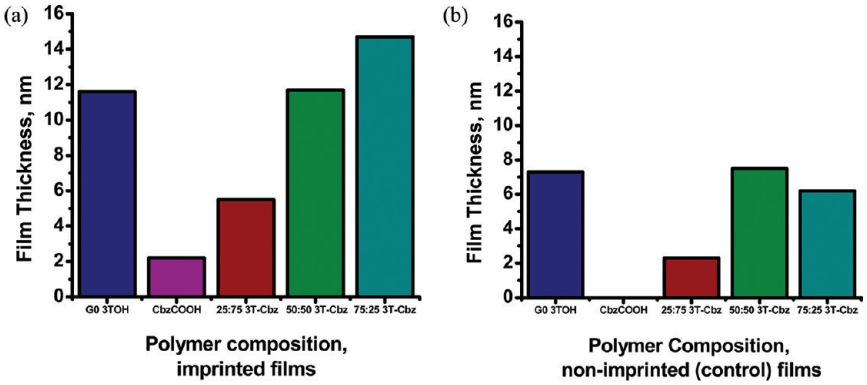

Figure 4. Different thickness of the (a) imprinted and (b) nonimprinted polymer films at various composition ratios as measured by ellipsometry.

with the desired amount of recognition sites and allow for facile release and rebinding of the template.[7,8] In a traditional bulk MIP polymerization, a cross-linker is incorporated to enable polymer network formation which could hold and maintain the cavities that were formed even after washing. In this study, it was ascertained that copolymerization of the two monomers brings about the same effect as that of the addition of a cross-linker. The −OH and −COOH terminal groups present in each monomer provide additional sites in which BPA could possibly interact noncovalently toward complex formation.

The film thickness of both imprinted and nonimprinted polymer films prepared from different monomer concentrations of G0 3TOH and CbzCOOH was determined using ellipsometry. Generally, thin films were obtained from the electropolymerization of imprinted films as shown in Figure 4. Imprinted polymer films have thicknesses ranging from 2 to 15 nm. The films were also evaluated by SPR, and the results for the different polymer compositions are summarized in Figure S11 of the Supporting Information. Results emphasized the important role of thickness on the consequent performance of the E-MIP copolymer films. Thin films generally give an indication of a better mass transport of the target analyte during template removal and template rebinding processes. The desired property of the imprinted films to rebind with BPA is dictated by the film's surface mass density and thickness as these will enhance the efficiency of template removal and will facilitate the penetration of the template molecules within the polymer film resulting to occupation of the preformed cavities. Chen et al.[45] demonstrated the influence of film thickness on the formation of the binding cavities for uric acid. They reported that an increased loading of poly(amine−imide) resulted in an increase in film thickness alongside with an increase in the number of template molecules that have been trapped within the polymer network. Therefore, we may also ascertain that the large difference in the film thickness between MIP and NIP films is related to the increase in the number of BPA molecules that have been trapped within the polymer network. Moreover, with more BPA/template molecules incorporated in the E-MIP film, nonhomogeneity of the layer thickness was also observed.[46]

The wetting properties of the electropolymerized films (contact angle measurements with water) vary with polymer composition and in the presence of the template. However, no clear trend was observed for films prepared in either the presence or absence of the template as the measured contact angle differs with varying polymer composition of the E-MIP film. Variations in the degree of polymerization of the individual monomer (terthiophene and carbazole) brought about by variations in the nucleating ability of each monomer in the presence and absence of the template molecules may be crucial. Yet, the data also shows that E-MIP films were generally hydrophobic than the NIP film surface as suggested by moderately higher contact angle values. These results imply that the fabricated E-MIP copolymer films have varying degree of hydrophobicity, which may have been influenced not only by the differences in the copolymer composition of the resulting films due to inter- and intrachain polymer interactions but also to the increase in the loading of the template molecules that have been trapped within the polymer network (commensurate to the distribution of functional groups during the polymer formation). This gives rise to additional intermolecular forces of attraction. This may be important in assessing the effect of nonspecific adsorption with these films. The results comparing the various thicknesses and their wetting properties are also summarized in the Supporting Information (Table S2).

The AFM images, shown in Figure S4 of the Supporting Information, display surface morphologies of the copolymer films, with and without the BPA molecules. The E-MIP film has relatively thicker surface compared to NIP as a result of the insertion of BPA molecules within the confines of the polymer network. Moreover, with the introduction of BPA molecules, there were more aggregates that have been formed and were visibly seen on the AFM images, which is possibly associated with the presence of additional intermolecular forces of attraction due to template−monomer interactions. This makes the surface of the E-MIP film rougher as compared with the nonimprinted film. This observation was also supported by the data obtained from water contact angle measurements, which indicate higher contact angle values (correspondingly, have higher surface energy and greater hydrophobicity) for the E-MIP film than the NIP. Based on Wenzel[47] and Cassie−Baxter[48] theories, the increase in contact angle of the surface is related to the increased in surface roughness. Furthermore, Marmur[49] suggested that the increase in the hydrophobicity is due to the increase in the heterogeneity of the surface.

It was also observed that the film thickness of the imprinted films was found to be dependent on the amount of G0 3TOH; that is, film thickness tends to increase with increasing concentration of the G0 3TOH in the polymer film. Thus, in addition to ellipsometry, surface plasmon resonance (SPR) analysis was conducted. SPR gives a highly sensitive response due to change in refractive index on the gold surface.[50] The resulting best fit (as calculated and then compared with the measured curves)

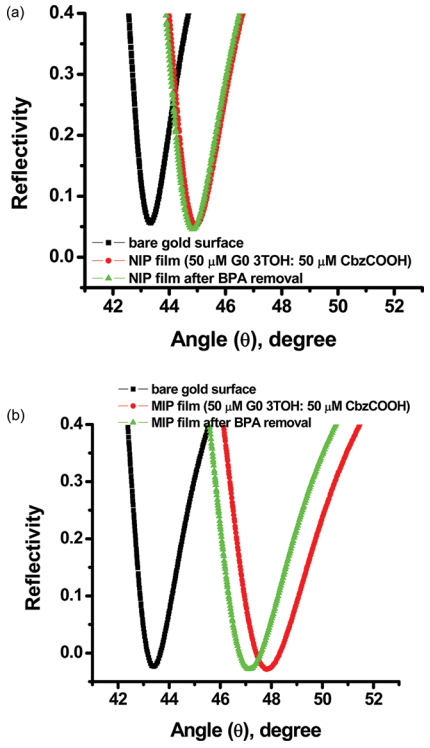

Figure 5. Observed shift in the minima of the SPR curve to higher angle in the presence of bisphenol A. SPR curves before and after electropolymerization and after template (BPA) removal: (a) nonimprinted film and (b) imprinted polymer film. SPR curve for bare gold was used as reference.

gives the optical thickness of the MIP film (see Supporting Information).[51]

A significant shift on the minima of the SPR curve as shown in Figure 5a,b was observed upon the electrochemical deposition of equimolar amounts of G0 3TOH and CbzCOOH on Au substrate, for both nonimprinted and BPA imprinted polymer films. This is indicative of a change in the dielectric constant of the dielectric layer on top of the gold surface upon the formation of the polymer film. Specifically, an increase in the resonance angle was observed upon the interaction of the electropolymerized G0 3TOH and CbzCOOH films with the template (BPA). The resonance angle shifted from 43.9° to 48° in the case of the MIP film against the observed shift from 43.8° to 45.1° for the electrodeposition of NIP film. Such shift on the minima of the SPR curves (but without affecting the reflectance of the SPR curves) reflects on the specific recognition between the binding sites of the E-MIP film and BPA as well as the successful incorporation of the template molecules within the polymer structure (BPA). This observation was further affirmed when the resonance angle decreased to 47.4° when the MIP film was subjected to washing with various solvents such as methanol: acetic acid (80:20 v/v), methanol, and acetonitrile to effect the removal of the template. However, the resonance angle of the nonimprinted G0 3TOH and CbzCOOH film only shifted by a mere 0.1°, i.e., from 45.1° to 45.0°. This minute shift can be ascribed to the weak and nonspecific adsorption due to the variation in the cross-linking/conformational arrangement of the copolymer film without the template. Figure 5a,b depicts the observed shift in the minima of the SPR curve after template washing for nonimprinted and MIP films, respectively. As such, the SPR results give a clear demonstration of the finite change in the thickness and/or refractive index of the polymer films with and without BPA as template. On the basis of experimental results and the fitting parameters employed during simulations using Winspall software (employing algorithms based on the above shown Fresnel equations), E-MIP film thickness depicts a change from 24.2 to 14.2 nm after BPA washing. On the other hand, template removal for the nonimprinted film renders the film thickness to vary from 9.1 to 7.2 nm.

Theoretical Modeling of the Polythiophene-*co*-polycarbazole−BPA Complexation. The efficiency and selectivity of the resulting E-MIP film are dictated by the number and the relative strength of the prepolymer complex or template−monomer interactions[52] and hence must be given utmost importance during the optimization stage of the polymerization process. Modeling studies could be an important tool in tandem with experimental results to envisage important structural or mechanistic information leading to the formation of high affinity sites in an electropolymerized terthiophene−carbazole E-MIP film.

The theoretical modeling studies were performed in order to predict the possible interactions of the monomers with BPA molecules through calculations of the stabilization energies of the resulting monomer−template complexes. The theoretical part of this study permits the visualization of such interactions, which aids us in identifying the plausible interplay of effects such as the nature of interaction of the monomers with the template upon the resulting sensory properties of the E-MIP copolymer film that we have observed from our experimental data. The theoretical model of the interactions of BPA molecules with different ratios of G0 3TOH and CbzCOOH was obtained from semiempirical PM3 calculations using Spartan 08 as shown in Figure 6. The model suggests the formation of preformed arrangement of the monomers and template within the network, which may be correlated to our assumption with regards to the insertion of BPA molecules within the polymer network during electrodeposition. The interaction energy between the monomers and template was obtained from calculated heats of formation using eq 2:

$$\Delta E = E_{\text{bisphenol A/G1 3TOH/CbzCOOH complex}} - [E_{\text{G0 3TOH}} + E_{\text{bisphenol A}} + E_{\text{CbzCOOH}}] \quad (2)$$

A negative value for ΔE denotes favorable interaction between the monomer and the target analyte.[53] The calculated interaction energy for such conformation or arrangement of the G0 3TOH/CbzCOOH−BPA complex, 1:3:1 ratio, is −35.9 kJ/mol, suggesting that a relatively stable complex is formed at a high molar ratio of the carbazole derivative, predicting a fairly good affinity of the BPA with the CbzCOOH functional monomer. As also predicted by the model shown in Figure 6, the proposed arrangement of molecules may have been made possible by an H-bonding interaction providing stability to the formed complex between G0 3TOH, CbzCOOH, and BPA. In particular, a favorable donor−acceptor H-bonding between the oxygen atoms in the HO- of the G0 3TOH monomer, the carboxyl moiety present in CbzCOOH, and the hydrogens of the hydroxyl groups of the template (bisphenol A) are possibly formed as implied by the calculated bond distances. The model predicts the formation of H-bonds if calculated bond distances (represented by broken lines) are less than or equal to 2.00 Å.

The interaction of excess amount of G0 3TOH with BPA and CbzCOOH cannot be discounted too as results of semiempirical calculations suggest that a relatively stable complex can also be

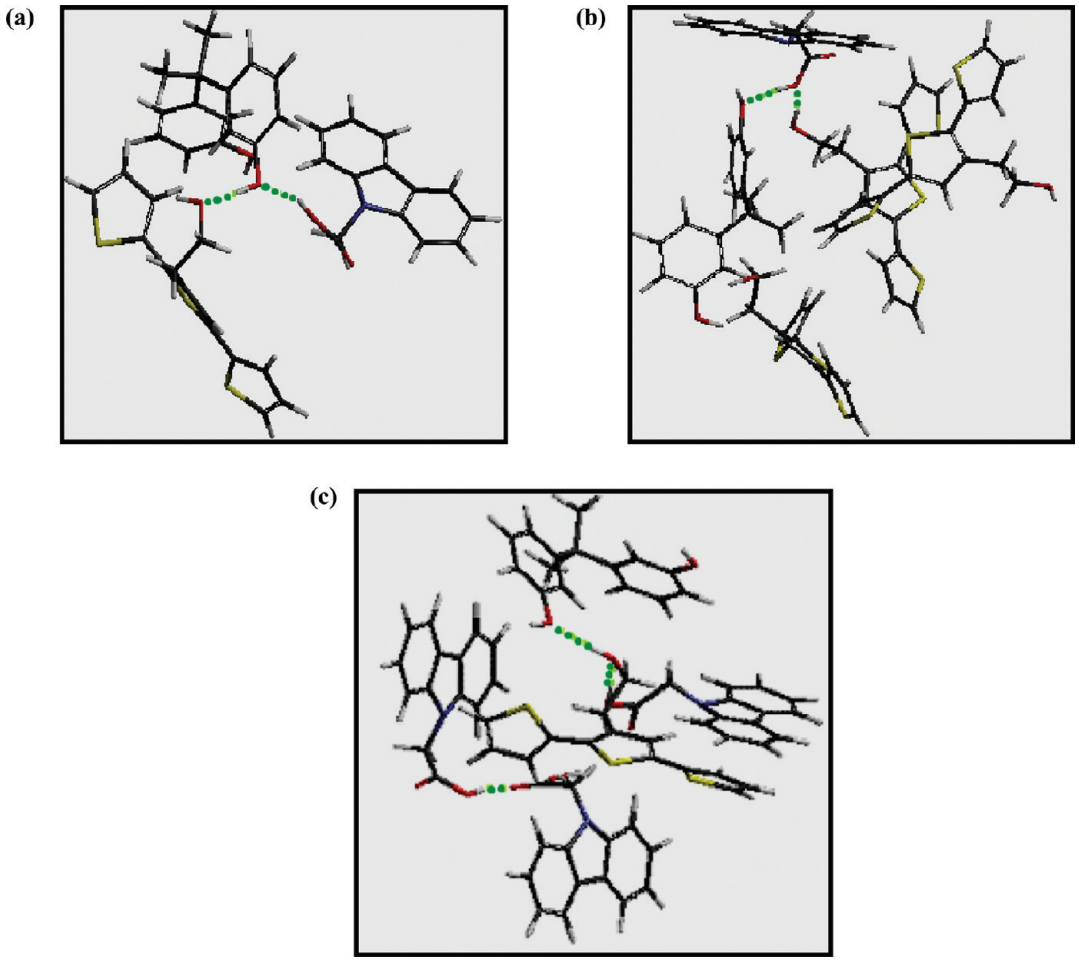

Figure 6. Predicted complex structure between bisphenol A and G0 3TOH and CbzCOOH monomers within the imprinted polymer matrix through PM3 semiempirical calculations using Spartan 08, Wavefunction, Inc.: (a) equimolar ratio of G0 3TOH-CbzCOOH; (b) 75:25 G0 3TOH-CbzCOOH; (c) 25:75 G0 3TOH-CbzCOOH.

formed giving a net stabilization energy for the complex equal to −24.3 kJ/mol. The disordered arrangement observed is caused by the random orientation of the monomer units. The reliability of the E-MIP film as a receptor may also be gauged by the relative flexibility of the template in the presence of functional monomers. The orientation of the template at each stage of E-MIP preparation, i.e., electropolymerization, solvent washing, and template rebinding, must have been preserved in order to attain high rebinding efficiency. In order to predict the changes on the conformation of BPA in the absence of the functional monomers (Figure 7), a single point energy calculation was performed. From such calculations, the angle generated by C-2 (phenyl ring 1), C-13 (tertiary carbon), and C-10 (phenyl ring 2) was measured and was used as reference to prefigure the extent of twisting that may have occurred to the two phenyl rings when in contact with monomer molecules. The angle obtained was 111.2°.

The results of the conducted modeling studies show that the bond angle varies with polymer composition. Semiempirical calculations show that the bond angle decreases upon interaction of BPA with 3:1 molar ratio of G0 3TOH:CbzCOOH. Nevertheless, it may be predicted from these calculations that as the amount of the functional monomer is increased, the bond angle between the phenyl rings has also increased. Theoretically, this demonstrates the interaction of the BPA with the functional monomers; with the two phenyl ring tend to pull away from each other due to hydrogen bond formation of the hydroxyl group attached to each phenyl ring. We presupposed that this was probably the most favorable conformation for the BPA to permit extensive interactions with the monomers, which may have explained for the observed progression of the electrochemistry of the thiophene−carbazole moieties in the presence of BPA during the electrochemical deposition as suggested by our CV data. In their study involving the preparation of imprinted polymer nanowires for protein binding, Li et al.[54] reported the same line of reasoning that protein molecules might have a precisely positioned amide group that permitted a multitude of simultaneous hydrogen bonds, which formed between the oriented amide groups within the binding site and the protein surface polar residues.

Template (BPA) Removal Studies by X-ray Photoelectron (XPS) and Fluorescence Spectroscopy. The XPS technique was used to confirm the successful incorporation of the template molecule on the imprinted polymer. XPS spectra were obtained from film samples electropolymerized on a gold-coated BK7 glass (Figure S7, Supporting Information). BPA was then removed from the imprinted polymer by dissolution in the following solvents—methanol/acetic acid (1:4, v/v) and acetonitrile—followed by washing with methanol and subsequently

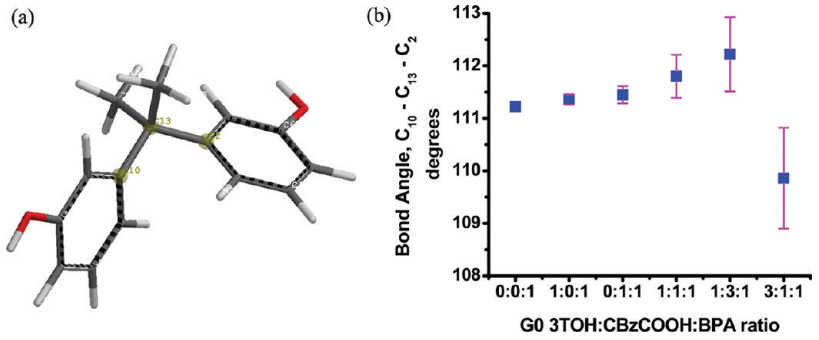

Figure 7. (a) Predicted conformation of bisphenol A generated after performing single point energy calculations, i.e., in the absence of the functional monomers. (b) Plot correlating calculated changes in the bond angle ($C_{10}-C_{13}-C_2$ of BPA) with varying polymer composition.

dried under a stream of nitrogen gas. Washing of the polymer film was repeatedly done for each solvent for a total washing time of 6.5 h. The NIP which served as control was also treated in the same way as the MIP. In the absence of an elemental marker on the template's structure, the high resolution scan for C 1s electron for imprinted film samples was used to determine the extent of BPA removal from the polymer films. C 1s electron signal from E-MIP film can be tracked at binding energy equal to 284 eV. A decrease in the number of counts per second indicates successful removal of BPA. Translating this decrease in the number of counts per second into atomic concentration of C 1s, the E-MIP film was found to contain ~81.08% C, whereas upon BPA removal, the atomic concentration for C 1s was found to be ~80.38%. Though high resolution scans for O 1s was not considered, per se, due to the presence of adventitious oxygen, it was also deemed relevant to obtain the ratio of O atom concentration with C atom concentration before and after template removal. Experimental results yield ~0.144 O 1s/C 1s ratio before BPA removal while approximately 0.116 O 1s/C 1s ratio was calculated after the release of the template from the E-MIP network. This clearly reinforces the results obtained from SPR measurements wherein it was shown that the film thickness diverged before and after template washing, which proved successful formation of binding cavities within the polymer network via the liberation of BPA molecules.

The film samples without template were subjected to fluorescence analysis (results summarized in Table S1 of the Supporting Information). Fluorescence is the emission which results from the return to the lower orbital of the paired electron.[55] Polythiophenes and polycarbazoles generally display significant fluorescence due to the presence of delocalized electrons present in conjugated double bonds. The relatively high fluorescence of these compounds can be explained by the position of the nonbonding orbital which is perpendicular to the plane of the ring, allowing it to overlap the p-orbitals on the adjacent carbon atoms.[56] Comparison of the emission intensities of the imprinted and nonimprinted polymer films after electropolymerization showed that BPA enhances the fluorescence emission of the polymer film. The observed enhancement may be attributed to the complexation of BPA with the copolymer facilitated by the formation of H-bonds arising from interactions of the −COOH group of the carbazole, −OH group of the G0 3TOH, and that of phenolic −OH groups of BPA.[57] The conformational flexibility of the cross-linked polymer film was assumed to have been further hindered due to the efficient trapping of BPA in the binding cavities within the polymer network.[58,59] Thus, successful template removal may be gauged by a decrease in the intensity. Table S1 (Supporting Information) provides a summary of the emission intensities obtained from imprinted and nonimprinted polymer films before and after template removal.

Evaluation of the Analytical Performance of the E-MIP Sensor by Electrochemical Impedance Spectroscopy (EIS). Electrochemical impedance spectroscopy was used to demonstrate the difference in the interfacial properties of conducting polymer films[60] deposited on the ITO substrate. Changes in the dielectric and electrical properties of the copolymer films during rebinding of BPA were investigated. Specifically, BPI imprinted and nonimprinted copolymers of G0 3TOH and CBzCOOH films were electrodeposited (CV) onto the surface of ITO. The potential was cycled from 0 to 1.1 V ten (10 cycles) times at scan rate of 50 mV/s. The respective electrical responses of the films were obtained using the Autolab Frequency Analyzer (Brinkmann). The impedance data (amplitude and the phase shift of the resulting current) were recorded at each frequency from 100 kHz to 0.01 Hz. A total of 50 points were collected for each impedance measurement. A sinusoidal potential modulation of 10 mV amplitude was superimposed on a constant dc potential (0 V) during impedance measurements. The data obtained were then fitted (minimum of 50 iterations) into a particular equivalent electrical circuit using the complex nonlinear least-squares (CNLS) admittance fitting program with the instrument. This is to obtain the following parameters: solution resistance (R_1), charge-transfer resistance (R_2), n, CPE, or differential capacitance (C_1). The Warburg circuit represented by $R_1(C_1[R_2W_1])$ may be used to describe the rebinding of BPA with the imprinted polymer films (Scheme 1 and Supporting Information). This equivalent circuit is preferentially used to model those modified surfaces with defects/channels for ion transport or adsorption. Components of the electrochemical polymer sensor system represented by the corresponding terms in the equivalent electrical circuit are as follows: (a) R_1, the ohmic resistance of the electrolyte solution; (b) R_2, the resistance of the polymer film layer; and (c) C_1, capacitor reflecting the properties of the double layer.

Electropolymerization of the imprinted films on the ITO surface resulted in changes on the electrochemical surfaces and that the behavior of NIP and E-MIP films can be differentiated using the EIS technique. The Nyquist plots, in which the imaginary impedance, Z'', is plotted against the real number, Z', are shown in Figure S8 of the Supporting Information. This type of plot provides information as to the nature of the

Scheme 1. Synthesis of G0 3TOH Terthiophene Dendron

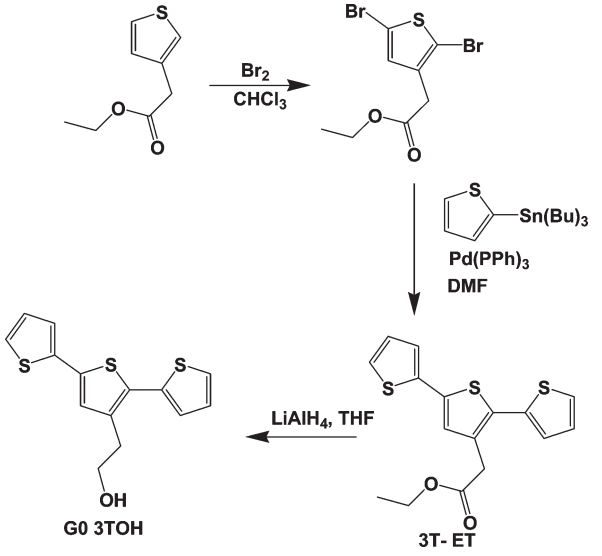

electrochemical process occurring at the electrode−electrolyte interface. The Nyquist plot indicates that the imprinted copolymer film exhibited both diffusion-related and charge-transfer-related processes, represented by the straight line and the semicircle region (green curve), respectively.[61] On the other hand, the nonimprinted copolymer exhibited only a diffusional-limited electrochemical process. Another useful plot from EIS analysis is the Bode phase plot, which gives information as to the relative insulating/conducting property of the polymer film. The Bode phase plots from the E-MIP and NIP films indicate that at lower frequencies the phase angles deviated from 90°, suggesting that the materials on the ITO surface are not free of defects. As a result, current leakage, through either ionic channels or electronic conduction exists.[62] This could be attributed to the intrinsic structure of the polymer film. This supports the assumption that the polymer films are permeable, which is an important property especially if the films are intended to be used for molecular recognition. Polymer film in sensors must act as a variable resistance to the passage of permeating molecules.[63]

The effect of the dc potential during impedance measurements as well as of time on the permeability of the imprinted G0 3TOH polymer film was also investigated. The applied dc potential was varied from +0.2 to −0.2 V, and the impedance spectra were obtained at each dc potential over a frequency range of 100 kHz to 0.01 Hz. As demonstrated in Figure S9 of the Supporting Information, it is evident that the total impedance of both the E-MIP and NIP polymer films increases as the electric potential is shifted toward the cathodic range, implying a reduction on the permeability of the polymer film brought about by minimal structural changes in the film. Interestingly, anodic shift of the electric potential causes the NIP film to be resistant to the penetration of ions or molecules. In contrast, the E-MIP film manifested a relatively good permeability at this potential range as indicated by the lower total impedance magnitude. Since the E-MIP films are electrochemically active, sensing of BPA was performed at 0 V dc potential, in which the polymer possesses an intermediate permeability. This is to prevent the films from undergoing structural changes brought about by the applied electric potential.

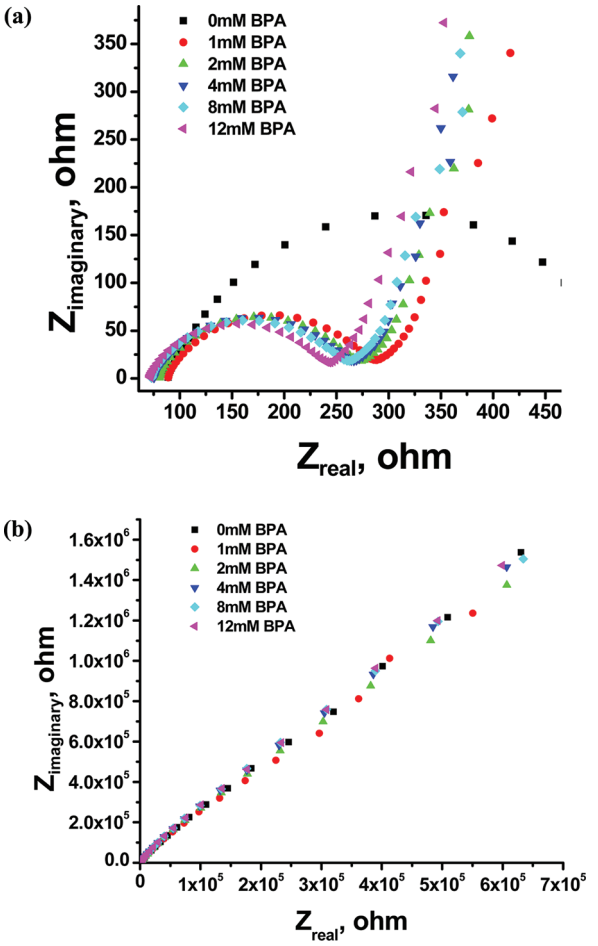

Figure 8. EIS response of (a) imprinted (E-MIP) G0 3TOH-CbzCOOH copolymer film and (b) nonimprinted (NIP) to bisphenol A.

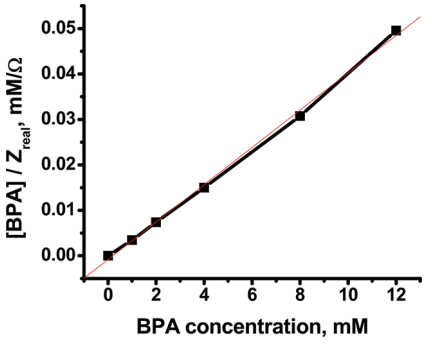

Figure 9. Dependence of the total impedance on increasing BPA concentrations: calibration plot of the BPA imprinted copolymer sensor.

Figure 8 depicts the distinct EIS response of the E-MIP against the NIP in sensing BPA, denoting successful imprinting. The E-MIP film was exposed to varying concentrations of BPA, i.e., from 0 to 12 mM, noting the change in the differential capacitance (C_1) at each concentration.[62] It can be observed from the Nyquist plots that the radii of the semicircles decrease linearly with increasing concentration of BPA. It is assumed that the template (bisphenol A) molecules were able to penetrate and bind with the cavities present within the imprinted polymer

dx.doi.org/10.1021/ma2010525 |*Macromolecules* 2011, 44, 6669–6682

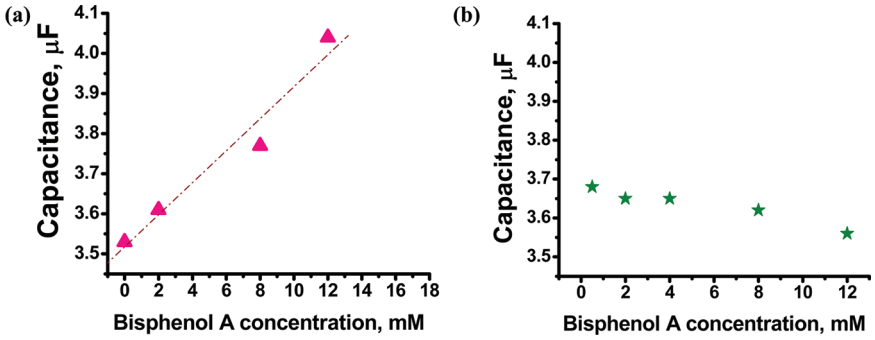

Figure 10. Plots depicting the observed variations on the capacitance of the imprinted (a) and nonimprinted polymer films (b) against increasing concentrations of the bisphenol A.

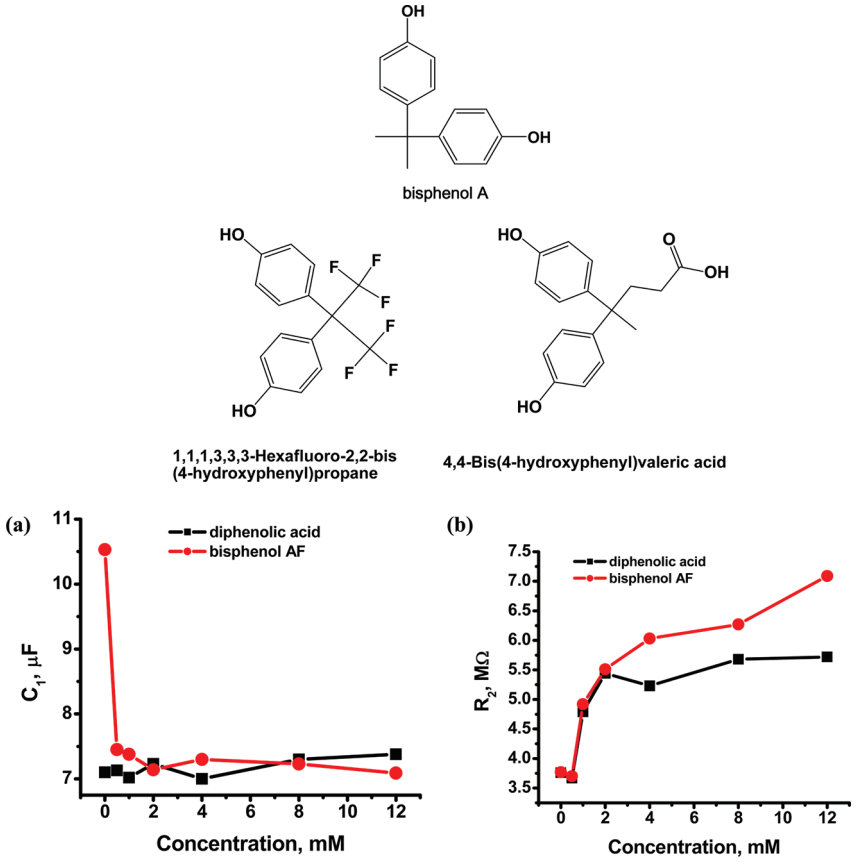

Figure 11. Observed changes in (a) capacitance and (b) charge-transfer resistance upon rebinding of bisphenol AF and diphenolic acid: demonstrating the relative selectivity of the imprinted polymer film toward bisphenol A. The chemical structures of the competing molecules are also shown.

network. On the other hand, the binding (or nonbinding) of BPA with the NIP did not result to any change in the impedance values. This provides support to the assumption that the NIP film was impermeable to ions or molecules.

The efficient trapping of BPA molecules in binding cavities within the E-MIP film caused the decrease on the electrochemical current brought about by an impediment in the flow of the electrons in an ac circuit. BPA molecules are assumed to have blocked the electrode surface and that the extent of such blockage is dependent on the concentration of BPA.[64] Changes in the total impedance obtained during the rebinding of the different concentrations of BPA on the imprinted film were used to calculate the amount of BPA using the equation of the line, [BPA]/ $Z = 0.00411[\mathrm{BPA}] - 0.00078$ ($R^2 = 0.9989$), as illustrated in Figure 9. Sensitivity of the sensor, which is a measure of its ability to discriminate between small differences in BPA concentration, was found to be equal to 0.004 11 Ω/mM. The limit of detection (LOD), which gives the minimum concentration of BPA that can be detected at a known confidence level, was calculated to be 0.42 mM.

As also demonstrated in Figure 10, differential capacitance of the E-MIP film was found to increase linearly with concentration of BPA. This denotes successful immobilization of BPA onto the cavities formed within the E-MIP sensor film. It is based on the assumption that the change in capacitance is due to the permeation of BPA molecules into the cavities formed within the film.[65]

dx.doi.org/10.1021/ma2010525 |*Macromolecules* 2011, 44, 6669–6682

Fairly good linearity (r^2 = 0.977 78) was obtained from the plot of differential capacitance with this concentration range of BPA. The observed changes on the capacitance can be correlated to the ratio of the dielectric constant to the thickness of the polymer film. The permeation of BPA may have resulted in the corresponding increase in the dielectric constant of the polymer film, causing the increase in capacitance values.[66] The eventual change in the thickness of the imprinted copolymer film upon rebinding of BPA may also be attributed to the changes in the structural properties such as porosity or mechanical of the copolymer films which usually accompanies the absorption process.[66] Both variables are associated with the packing structure of the polymer films deposited on the ITO surface. Jennings et al.[66] attributed higher packing density and conformational order to surfaces possessing (a) a smaller dielectric constant due to the exclusion of polar solvent molecules from the hydrophobic surface and (b) a thicker film due to a correspondingly smaller tilt angle.

Recognition Selectivity of BPA Imprinted Polymer. The selectivity of the BPA-imprinted polymer was investigated by exposing the E-MIP polymer film to increasing concentrations of bisphenol AF and diphenolic acid. The structures of these compounds are similarly related to that of the structure of bisphenol A. Diphenolic acid has a carboxylic acid group while bisphenolic AF contains several fluorine atoms. Their chemical structures are shown in Figure 11. EIS data show that there was a dramatic change in the electric response of the polymer films to these competing molecules. The polymer films used for this experiment manifested insulating properties as displayed in the Bode phase and total impedance magnitude plots shown in Figure S7 of the Supporting Information. Hence, the films can be regarded as near-ideal capacitor, and thus the data pertaining to capacitance and charge transfer resistance can be obtained by fitting it to a simple series $R_1(R_2C_1)$ equivalent circuit. The Nyquist plots of bisphenolic AF and diphenolic acid are more similar to the NIP films. Unlike the Nyquist plots of the BPA which showed that the radii of the semicircles decrease linearly with increasing concentration of BPA, these plots showed only a straight plot with some deviation in linearity at lower concentrations (Figure 12). It is assumed that only the original template (bisphenol A) molecules were able to penetrate and bind with the cavities present within the imprinted polymer network. On the other hand, the binding (or nonbinding) of bisphenolic AF and diphenolic acid with the E-MIP resulted only in a very small change in the impedance values unlike with the original BPA template (Figure 8). This provides support to the assumption that the E-MIP film was impermeable to these analogous molecules.

Comparing the response of the bisphenol A-selective E-MIP/EIS sensor to bisphenol AF and diphenolic acid as competing analogues, it can be derived from Figures 11 and 12 that the polymer film's capacitance did not change in the presence of increasing concentrations of these analogues. However, the capacitance values obtained after the rebinding of these analogues were found to be higher than the capacitance values obtained from the rebinding of BPA. This suggests the possible occurrence of some nonselective binding as the films exhibited a small resistance to penetration of these analogues.

The charge transfer resistance noted during the binding of the competing molecules accounts for the inherent electrochemical activity of the polymer film. This could represent some of the diffusion-limited processes occurring at the polymer film—electrode interface. The plot of charge-transfer resistance versus

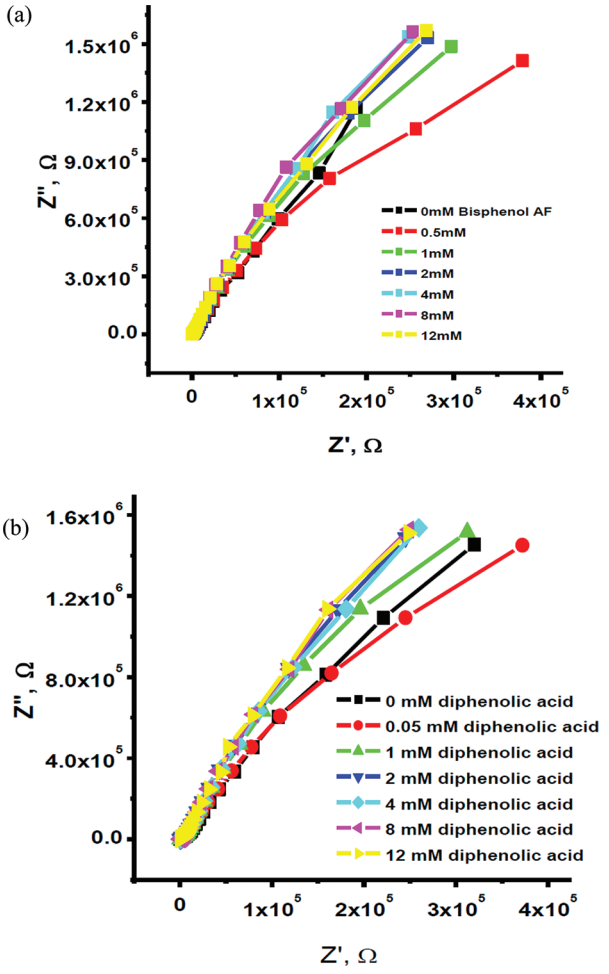

Figure 12. Observed changes in impedance upon rebinding of (a) bisphenol AF and (b) diphenolic acid on the templated BPA E-MIP copolymer film: demonstrating the relative selectivity of the imprinted polymer film toward BPA.

concentrations of the diphenolic acid indicates nonselective binding at lower concentrations ranging from 0 to 2 mM concentration (Figure 11). As the concentration was increased, the inability of the film to recognize diphenolic acid becomes more prominent as indicated by an almost constant charge transfer resistance. On the other hand, bisphenol AF can be a potential competitor for the binding of BPA at this concentration range as suggested by the linear plot of charge-transfer resistance against increasing concentrations of BPA. The charge-transfer resistance value obtained for the rebinding of bisphenol AF was found to be higher than the charge-transfer resistance obtained from the rebinding of BPA. Still, this is indicative of a more efficient rebinding of the original templated BPA molecules to the imprinted polymer surface since the bisphenol AF did not exhibit both diffusion-related and charge-transfer-related processes.

Thus, it was demonstrated that the polymer E-MIP films exhibited preference to the original BPA template over bisphenol AF and diphenolic acid and that the EIS techniques has been demonstrated to be an effective technique in assessing the interfacial properties of the E-MIP as well as functioning as a sensor with very good sensitivity and selectivity figures of merit.

CONCLUSIONS

We have demonstrated the application of electrochemical impedance spectroscopy (EIS) in an artificial chemical receptor prepared as E-MIP using electropolymerizable terthiophene and carbazole monomers for the imprinting of bisphenol A, a known endocrine disrupting chemical. The copolymers of bifunctional monomers of −COOH from the carbazole derivative and −OH functional group from terthiophene were found to possess good molecular recognition properties than when these respective monomers were singly electropolymerized. As in any electropolymerized films for sensing applications, a compromise of thickness and efficient formation of pre polymer complexes must be achieved in order to ensure maximum rebinding of the template molecules. Cyclic voltammetry offers a simple means of depositing sensor films directly onto substrate surfaces while the EIS techniques provides a versatile means of measuring the amount of template bound to the polymer matrix. Moreover, in this study, the EIS has been demonstrated to give extensive information related to the permeability and thickness of the polymer material deposited on the surface that may be used in advancing technologies relating to sensing via reversible surfaces through electric potential control and to development of dynamic surfaces for advanced sensing technology.

ASSOCIATED CONTENT

Supporting Information. XPS spectra, tabulated fluorescence data, other Nyquist and Bode plots obtained from EIS sensing, etc. This material is available free of charge via the Internet at http://pubs.acs.org.

AUTHOR INFORMATION

Corresponding Author
*E-mail: radvincula@uh.edu. Phone: +1 713 743 1760.

ACKNOWLEDGMENT

The authors acknowledge funding from the National Science Foundation CBET-0854979, DMR-10-06776, and Robert A. Welch Foundation, E-1551. We also acknowledge contribution from Amani Kawach. D.C.A. gratefully acknowledges the DOST-Philippine Council for Industry, Energy and Emerging Technology Research (PCIEERD) and the Mines and Geosciences Bureau-Department of Environment and Natural Resources (MGB-DENR) for financial support. We also acknowledge technical support from Inficon Inc, Biolin/Attension, Metrohm, Optrel GbR, and Agilent Technologies.

REFERENCES

(1) Yoshida, T.; Horie, M.; Hoshino, Y.; Nakazawa, H. *Food Addit. Contam.* **2001**, *18*, 69–75.
(2) Cao, X.-L.; Corriveau, J.; Popovic, S. *J. Agric. Food Chem.* **2009**, *57*, 1307–1311.
(3) Malitesta, C.; Losito, I.; Zambonin, P. G. *Anal. Chem.* **1999**, *71*, 1366–1370.
(4) Dickert, F. L.; Hayden, O.; Halikias, K. P. *Analyst* **2001**, *126*, 766–771.
(5) Piletsky, S. A.; Terpetschnig, E.; Andersson, H. S.; Nicholls, I. A.; Wolfbeis, O. S. *Fresenius J. Anal. Chem.* **1999**, *364*, 512–516.
(6) Lin, J. M.; Yamada, M. *Analyst* **2001**, *126*, 810–815.
(7) Apodaca, D.; Pernites, R.; Ponnapati, R.; Del Mundo, F.; Advincula, R. *ACS Appl. Mater. Interfaces* **2011**, *3*, 191–203.
(8) (a) Pernites, R.; Ponnapati, R.; Advincula, R. *Macromolecules* **2010**, *43*, 9724–9735. (b) Pernites, R.; Ponnapati, R.; Felipe, J.; Advincula, R. *Biosens. Bioelectron.* **2011**, *26*, 2766–2771.
(9) Wu, X.; Shimizu, K. D. In *Molecular Recognition and Polymers: Control of Polymer Structure and Self-Assembly*; Rotello, V., Thayumanavan, S., Eds.; John Wiley and Sons: Hoboken, NJ, 2008; p 397.
(10) Schweitz, L. *Anal. Chem.* **2002**, *74*, 1192–1196.
(11) Shibayama, K.; Seidel, S. W.; Novak, B. M. *Macromolecules* **1997**, *30*, 3159–3163.
(12) Sellergren, B.; Ruckert, B.; Hall, A. J. *Adv. Mater.* **2002**, *14*, 1204–1208.
(13) Malitesta, C.; Losito, I.; Zambonin, P. G. *Anal. Chem.* **1999**, *71*, 1366–1370.
(14) Foulds, N. C.; Lowe, C. R. *J. Chem. Soc., Faraday Trans. 1* **1986**, *82*, 1259–1264.
(15) Guo, M.; Chen, J.; Zhang, Y.; Chen, K.; Pan, C.; Yao, S. *Biosens. Bioelectron.* **2008**, *23*, 865–871.
(16) Zhang, J.; Lei, J.; Pan, R.; Xue, Y.; Ju, H. *Biosens. Bioelectron.* **2010**, *26*, 371–375.
(17) Choi, S.-W.; Chang, H.-J.; Lee, N.; Kim, J.-H.; Chun, H. S. *J. Agric. Food Chem.* **2009**, *57*, 1113–1118.
(18) Taranekar, P.; Fulghum, T.; Baba, A.; Patton, D.; Advincula, R. *Langmuir* **2007**, *23*, 908–917.
(19) Nalwa, H. S., Ed. *Handbook of Organic Conductive Molecules and Polymers*; John Wiley and Sons: New York, 1997.
(20) Roncali, J. *Chem. Rev.* **1992**, *92*, 711–738.
(21) (a) Welzel, H. P.; Kossmehl, G.; Schneider, J.; Plieth, W. *Macromolecules* **1995**, *28*, 5575–5580. (b) Zhang, W.; Dong, S. *J. Electroanal. Chem.* **1990**, *284*, 517–521. (c) Atta, N. F.; Galal, A.; Karagozler, A. E.; Russell, G. C.; Zimmer, H.; Mark, H. B. *Biosens. Bioelectron.* **1991**, *6*, 333–341.
(22) (a) Hoegl, H.; Su, O.; Neugebauer, W. EU Patent 1068115, 1957. (b) Hoegl, H. *J. Phys. Chem.* **1965**, *69*, 755–766.
(23) Koyuncu, S.; Kaya, I.; Koyuncu, F. B.; Ozdemir, E. *Synth. Met.* **2009**, *159*, 1034–1042.
(24) (a) Grazulevicius, J. V.; Strohriegl, P.; Pelichowski, J.; Pelichowski, K. *Prog. Polym. Sci.* **2003**, *28*, 1297–1353. (b) Grigoras, M.; Antonia, M. C. *Eur. Polym. J.* **2005**, *41*, 1079–1089. (c) Kimoto, A.; Cho, J. S.; Higuchi, M.; Yamamoto, K. *Macromolecules* **2004**, *37*, 5531–5537. (d) Stephan, O.; Vial, J.-C. *Synth. Met.* **1999**, *106*, 115–119.
(25) Schopf, G. Kossmehl, G. *Polythiophenes-Electrically Conductive Polymers*; Springer: Berlin, 1995.
(26) Taranekar, P.; Baba, A.; Fulghum, T. M.; Advincula, R. C. *Macromolecules* **2005**, *38*, 3679–3687.
(27) (a) Blanco-Lopez, M. C.; Lobo-Castanon, M. J.; Miranda-Ordieres, A. J.; Tunon-Blanco, P. *Trends Anal. Chem.* **2004**, *23*, 36–48. (b) Piletsky, S. A.; Turner, A. P. F. *Electroanalysis* **2002**, *14*, 317–323. (c) Henry, O. Y. F.; Cullen, D. C.; Piletsky, S. A. *Anal. Bioanal. Chem.* **2005**, *382*, 947–956.
(28) Sellergren, B. *Molecularly Imprinted Polymers: Man-made Mimics of Antibodies and their Applications in Analytical Chemistry*; Elsevier: Amsterdam, 2000.
(29) (a) Bi, X.; Yang, K. *Anal. Chem.* **2009**, *81*, 527–532. (b) Jenik, M.; Schirhagl, R.; Schirk, C.; Hayden, O.; Lieberzeit, P.; Blaas, D.; Paul, G.; Dickert, F. L. *Anal. Chem.* **2009**, *81*, 5320–5326. (c) Alexander, C.; Andersson, H. S.; Andersson, L. I.; Ansell, R. J.; Kirsch, N.; Nicholls, I. A.; O'Mahony, J.; Whitcombe, M. J. *J. Mol. Recognit.* **2006**, *19*, 106–180. (d) Jiang, G.; Baba, A.; Advincula, R. *Langmuir* **2007**, *23*, 817–825.
(30) Millan, M. D.; Locklin, J.; Fulghum, T.; Baba, A.; Advincula, R. C. *Polymer* **2005**, *46*, 5556–5568.
(31) (a) Cao, C. N. *Electrochim. Acta* **1990**, *35*, 831–836. (b) Liu, M.; Zhang, Y.; Wang, M.; Deng, C.; Xie, Q.; Yao, S. *Polymer* **2006**, *47*, 3372–3381.
(32) Ponnapati, R.; Felipe, M. J.; Park, J. Y.; Vargas, J.; Advincula, R. C. *Macromolecules* **2010**, *43*, 10414–10421.

(33) Taranekar, P.; Fulghum, T.; Baba, A.; Patton, D.; Ponnapati, R.; Clyde, G.; Advincula, R. *J. Am. Chem. Soc.* **2007**, *129*, 12537–12548.
(34) (a) Ulman, A. *An Introduction to Ultrathin Organic Films: From Langmuir-Blodgett to Self Assembly*; Academic: New York, 1991. (b) Sullivan, J. T.; Harrison, K. E.; Mizzell, J. P., III; Kilbey, S. M., II *Langmuir* **2000**, *16*, 9797–9803.
(35) Taranekar, P.; Park, J. Y.; Patton, D.; Fulghum, T.; Ramon, J. G.; Advincula, R. C. *Adv. Mater.* **2006**, *18*, 2461–2465.
(36) Sezer, E.; Hooren, V. M.; Sarac, S. A.; Hallensleben, L. M. *J. Polym. Sci., Part A: Polym. Chem.* **1999**, *37*, 379–381.
(37) Back, M. G.; Stevens, R. C.; Charych, D. H. *Bioconjugate Chem.* **2000**, *11*, 777–788.
(38) Faid, K.; Leclerc, M. *J. Chem. Soc., Chem. Commun.* **1996**, 2761–2762.
(39) (a) Vanden Bout, D. A.; Yip, W. T.; Hu, D.; Fu, D. K.; Swager, T. M.; Barbara, P. F. *Science* **1997**, *277*, 1074. (b) Hu, D.; Yu, J.; Wong, K.; Bachi, B.; Rossky, P. J.; Barbara, P. F. *Nature* **2000**, *405*, 1030.
(40) Yang, A.; Kuroda, M.; Shiraishi, Y.; Kobayashi, T. *J. Chem. Phys.* **1998**, *109*, 8442–8550.
(41) (a) Otero, T. F.; Grande, H.; Rodriguez, J. *Electrochim. Acta* **1996**, *41*, 1863–1869. (b) Otero, T. F.; Boyano, I. *J. Phys. Chem. B* **2003**, *107*, 6730–6738.
(42) Sauerbrey, G. *Z. Phys.* **1959**, *155*, 206–222.
(43) Bauerle, P.; Gotz, G.; Hiller, M.; Scheib, S.; Fischer, T.; Segelbacher, U.; Bennati, M.; Grupp, A.; Mehring, M.; Stoldt, M.; Seidel, C.; Geiger, F.; Schweiger, H.; Umbach, E.; Schmelzer, M.; Roth, S.; Egelhaaf, H. J.; Oelkrug, D.; Emele, P.; Port, H. *Synth. Met.* **1993**, *61*, 71–79.
(44) Yilmaz, E.; Mosbach, K.; Haupt, K. *Anal. Commun.* **1999**, *36*, 167–170.
(45) Chen, P.-Y.; Vittal, R.; Nien, P.-C.; Lion, G-S.; Ho, K.-C. *Talanta* **2010**, *80*, 1145–1151.
(46) Jakusch, M.; Janotta, M.; Mizaikoff, B. *Anal. Chem.* **1999**, *71*, 4786–4791.
(47) Wenzel, R. W. *Ind. Eng. Chem.* **1936**, *28*, 988–994.
(48) Cassie, B. D.; Baxter, S. *Trans. Faraday Soc.* **1944**, *40*, 546–551.
(49) Marmur, A. *Langmuir* **2003**, *19*, 8343–8348.
(50) Choi, S. W.; Chang, H. J.; Lee, N.; Kim, J. H.; Chun, H. S. *J. Agric. Food Chem.* **2009**, *57*, 1113–1118.
(51) Knoll, W. *Annu. Rev. Phys. Chem.* **1998**, *49*, 569–638.
(52) Andersson, H. S.; Koch-Schmidt, A. C.; Ohlson, S.; Mosbach, K. *J. Mol. Recognit.* **1996**, *9*, 675–682.
(53) (a) Holdsworth, C. I.; Bowyer, M. C.; Lennard, C.; McCluskey, A. *Aust. J. Chem.* **2005**, *58*, 315–320. (b) Schwarz, L.; Bowyer, M. C.; Holdsworth, C. I.; McCluskey, A. *Aust. J. Chem.* **2006**, *59*, 129–134. (c) Schwarz, L.; Holdsworth, C. I.; McCluskey, A.; Bowyer, M. C. *Aust. J. Chem.* **2004**, *57*, 759–764.
(54) Li, Y.; Yang, H.; You, Q.; Zhuang, Z.; Wang, X. *Anal. Chem.* **2006**, *78*, 317–320.
(55) Lakowicz, J. R. *Principles of Fluorescence Spectroscopy*; Plenum Press: New York, 1983.
(56) Valeur, B. *Molecular Fluorescence: Principles and Applications*; Wiley-VCH: Verlag GmbH, 2001.
(57) Konishi, K.; Takase, E.; Fukunaga, N. *Langmuir* **2011**, *27*, 1332–1335.
(58) Tazuke, S.; Guo, R. K.; Hayashi, R. *Macromolecules* **1988**, *21*, 1046–1051.
(59) Hu, R.; Lager, E.; Aguilar, A. A.; Liu, J.; Lam, J. W. Y.; Sung, H. H. Y.; Williams, I. D.; Zhong, Y.; Wong, K. S.; Peña-Cabrera, E.; Tang, B. Z. *J. Phys. Chem. C* **2009**, *113*, 15845–15853.
(60) Gu, H.; di Su, X.; Loh, K.-P. *J. Phys. Chem. B* **2005**, *109*, 13611–13618.
(61) Katz, E.; Willner, I. *Electroanalysis* **2003**, *15*, 913–947.
(62) Wang, W.; Zhang, S.; Chinwangso, P.; Advincula, R. C.; Lee, T. R. *J. Phys. Chem. C* **2009**, *113*, 3717–3725.
(63) Dong, H.; Cao, X.; Li, C. M. *ACS Appl. Mater. Interfaces* **2009**, *1*, 1599–1606.
(64) Park, J.-Y.; Lee, Y-S.; Kim, B. H.; Park, S.-M. *Anal. Chem.* **2008**, *80*, 4986–4993.
(65) Sharma, R.; Henderson, C.; Warren, G. W.; Burkett, S. L. *J. Appl. Polym. Sci.* **1998**, *68*, 553–560.
(66) Jennings, G. K.; Munro, J. C.; Yong, T.-H.; Laibinis, P. E. *Langmuir* **1998**, *14*, 6130–6139.